CORONAL PROPERTIES OF ACTIVE G-TYPE STARS IN DIFFERENT EVOLUTIONARY PHASES

L. Scelsi[1], A. Maggio[2], G. Peres[1], and R. Pallavicini[2]

[1]Dipartimento di Scienze Fisiche ed Astronomiche, Sezione di Astronomia, Università di Palermo, Piazza del Parlamento 1, 90134 Palermo, Italy

[2]INAF - Osservatorio Astronomico di Palermo, Piazza del Parlamento 1, 90134 Palermo, Italy

Abstract

We report on the analysis of XMM-*Newton* observations of three G-type stars in very different evolutionary phases: the "weak-line" T Tauri star HD 283572, the Zero Age Main Sequence star EK Dra and the Hertzsprung-gap giant star 31 Com. The X-ray luminosities of the three stars are all in the range $10^{30}-10^{31}$ erg/s. We compare the Emission Measure Distributions of these bright sources, derived from high-resolution X-ray spectra, as well as the pattern of elemental abundances vs. First Ionization Potential (FIP). The results of our analysis suggest that the coronae of these stars are very similar in terms of dominant coronal magnetic structures, in spite of differences in their evolutionary phases, surface gravities and metallicities.

Key words: X-rays: stars – techniques: spectroscopic – stars: activity – stars: coronae – stars: individual: 31 Com – stars: individual: EK Dra – stars: individual: HD 283572

1. Introduction

The analysis of high-resolution EUV and X-ray spectra of late-type stars, obtained with EUVE, XMM-*Newton* and *Chandra*, revealed that the thermal structure of coronal plasmas is well described by a continous Emission Measure Distribution vs. temperature, EMD, and that active stars have hotter and more isothermal coronae than low-activity stars (see, for example, the reviews by Bowyer et al 2000 and Favata & Micela 2003). Since the coronal plasma is optically thin, the EMD of the whole stellar corona can be used to study the properties of the coronal structures, where the plasma is magnetically confined.

In this work we have analyzed XMM-*Newton* spectra of three high-luminousity G-type stars in different evolutionary phases, HD 283572, EK Dra and 31 Com, with the aim of understanding whether the luminosity or the surface flux determines the characteristics of the EM distribution, or whether additional parameters like surface gravity or evolutionary phase also play a role.

2. The sample

HD 283572 is a bright X-ray source ($L_{\rm X} \sim 9\times10^{30}$ erg/s), belonging to the Taurus-Auriga star forming region, with an estimated age $\sim 10^7$ yr. It is a $2\,{\rm M}_\odot$ "weak-line" T Tauri star, which shows no signs of accretion from a disk.

EK Dra is a G1.5 star with nearly solar mass and radius, which has just arrived on the main sequence (age $\sim 7\times10^7$ yr). Its X-ray luminosity is $L_{\rm X} \sim 10^{30}$ erg/s.

The more massive ($M \sim 3\,{\rm M}_\odot$) giant star 31 Com has already evolved out of the main sequence and it is now crossing the Hertzsprung-gap in the H-R diagram. In this phase, 31 Com has developed a convective subphotospheric layer and a dynamo, giving rise to a corona with $L_{\rm X} \sim 7\times10^{30}$ erg/s. A detailed analysis of this star is reported in Scelsi et al (2004).

In Figure 1 we plot the positions of the sample stars in the H-R diagram, to show their respective evolutionary phases, while we report the stellar parameters in Table 1.

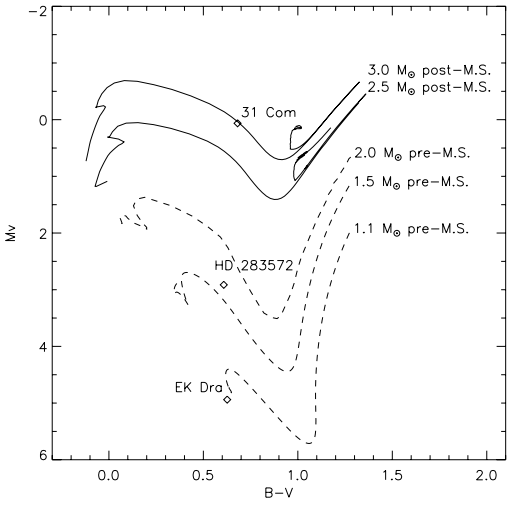

Figure 1. Positions of HD 283572, EK Dra and 31 Com in the H-R diagram. Dashed lines are pre-main sequence evolutionary tracks, while solid lines refer to post-main sequence tracks.

Table 1. Stellar parameters. Mass, radius, spectral type, projected rotational velocity and rotation period. Distances are measured by Hipparcos; L_x $(0.3-8$ keV$)$ are derived in this work from $3-T$ models; gravities are determined from the corresponding M and R values, and surface fluxes from the corresponding L_X and R values.

	$M/M_\odot$	$R/R_\odot$	Spectral type	$v \sin i$ (Km/s)	P_{rot} (d)	d (pc)	L_X (10^{30} erg/s)	$g/g_\odot$	F_X (10^6 erg s^{-1} cm^{-2})
HD 283572	1.8	2.7; 4.1 [a]	G2	78	1.55	128	~ 9	0.25; 0.12	20; 9
EK Dra	1.1	0.95	G1.5V	17.3	2.75	34	~ 1	1.2	18
31 Com	3	9.3	G0III	66.5	< 7.2 [b]	94	~ 7	0.035	1.3

[a] The two values are derived, respectively, through the Barnes-Evans relation (Walter et al 1987) and the *Hipparcos* estimate of d, and using Doppler imaging technique (Strassmeier & Rice 1998). [b] From $v \sin i$ and P_{rot}.

Table 2. Log of the XMM-Newton *observations.*

	EPIC pn Mode/Filter	Exposure time[a] (ks) pn	RGS1	RGS2	Count-rate[b] (s^{-1}) pn	RGS1	RGS2
HD 283572	Full Fr./Medium	41.1	0	47.4	2.20	0	0.15
EK Dra	Large Win./Thick	38.5	44.9	43.6	2.20	0.16	0.22
31 Com	Full Fr./Thick	32.2	39.6	38.5	1.45	0.11	0.16

[a] Excluding time intervals affected by proton flares, occurred in the cases of HD 283572 and 31 Com, and by a source flare in the case of EK Dra.
[b] Mean count-rate in the $0.2-10$ keV band for pn and in the $5-38$ Å band for RGS.

3. Observations

The observations of HD 283572, EK Dra and 31 Com were performed with XMM-*Newton* respectively on September, 5, 2000 (PI: R. Pallavicini), on December, 30, 2000 (PI: A. Brinkman) and on January 9, 2001 (PI: Ph. Gondoin). For the present study, we have considered only the EPIC/pn and RGS data; in Table 2 we report details on the instrument configurations and on the observations. Note that we have excluded from our analysis the time interval (~ 10 ks) of a flare on EK Dra.

4. EPIC pn spectra and 3-T model fitting

Photons were extracted from a circular region ($\sim 50''$ radius) within CCD 4 for HD 283572, while we used annular regions ($\sim 7.5'' - 50''$ radii) for 31 Com and EK Dra, to avoid pile-up effects. In all cases, background photons were extracted from the rest of CCD 4, excluding the sources and their out-of-time events. Figure 2 shows the background-subtracted pn spectra of the sample stars with their relevant best-fit models (see below).

EPIC pn spectra have been globally fitted in XSPEC v11.2 with multi-component thermal models based on the Astrophysical Plasma Emission Database (APED/ ATOMDB V1.2), in the $0.3-8$ keV band.

We found that an absorbed, optically-thin plasma with three isothermal components and variable element abundances provides an acceptable description of each of the pn spectra. The best-fit models are shown in Table 3, where the abundances are relative to the solar photospheric ones (Grevesse et al 1992). The abundances of the elements whose line complexes were not clearly detectable were tied to that of iron. To fit the spectra of EK Dra and 31 Com, we have also fixed the interstellar absorption at the values measured, respectively, by Güdel et al. (1997) and Piskunov et al (1997).

5. RGS spectra and EMD reconstruction

The background-subtracted RGS1 and RGS2 spectra have been rebinned on the same wavelength grid (bin size 0.02 Å) and co-added (Figure 3). We adopted a Lorentzian profile with variable width to measure line fluxes, and we estimated the continuum level independently with 3-T models best-fitting the EPIC pn spectra.

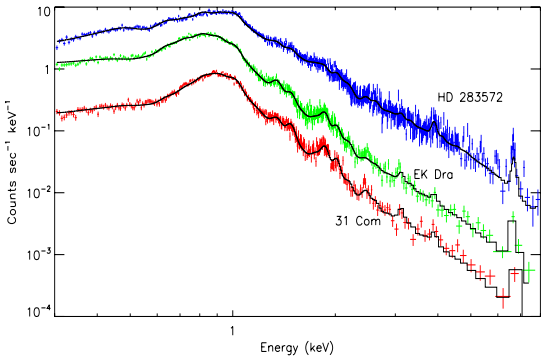

Figure 2. EPIC pn spectra of the three stars and best-fit models. The spectra of 31 Com and HD 283572, with their relevant models, have been shifted by -0.5 and +0.5 dex for purpose of illustration.

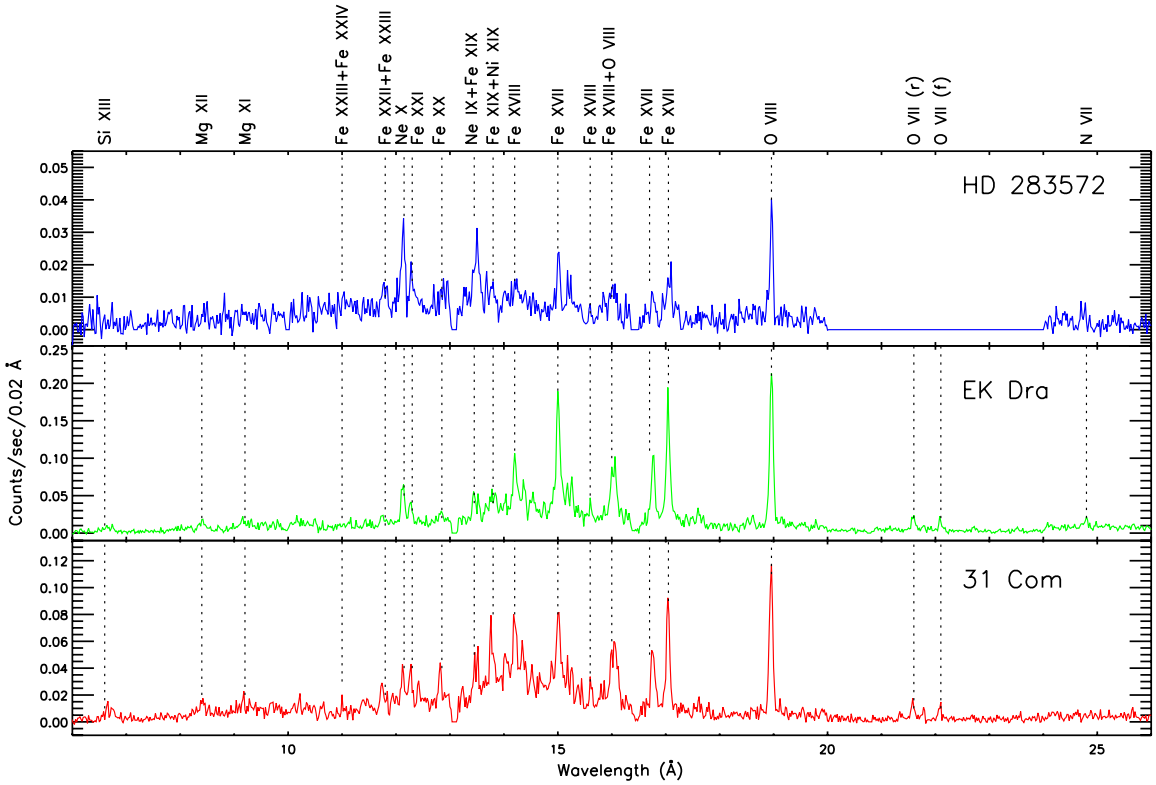

Figure 3. Co-added RGS spectra with the identification of the most prominent lines.

Table 3. Best-fit models of pn data with 90% statistical confidence ranges computed for one interesting parameters at a time; nominal errors on T_i and EM_i are at the 10% level. Parameters without errors were kept fixed.

	HD 283572	EK Dra	31 Com
$\log T_{1,2,3}$ (K)	6.64, 7.04, 7.43	6.58, 6.94, 7.33	6.44, 6.92, 7.28
$\log EM_{1,2,3}$ (cm^{-3})	53.5, 53.5, 53.7	52.5, 52.4, 52.3	52.6, 53.1, 53.0
$\log < T >$ (K)	7.21	6.99	7.06
C	= Fe	= 0.7 Fe	= 0.25 Fe
N	= Fe	= 0.5 Fe	= Fe
O	0.236 ± 0.014	0.346 ± 0.015	0.58 ± 0.03
Ne	0.46 ± 0.03	0.83 ± 0.04	2.35 ± 0.14
Mg	0.32 ± 0.05	0.86 ± 0.06	1.95 ± 0.13
Si	0.25 ± 0.04	0.59 ± 0.06	1.23 ± 0.11
S	0.26 ± 0.09	0.15 ± 0.10	0.58 ± 0.20
Ar	= Fe	0.82 ± 0.22	= Fe
Ca	1.8 ± 0.3	= Fe	= Fe
Fe	0.37 ± 0.01	0.83 ± 0.01	1.54 ± 0.02
Ni	1.52 ± 0.11	1.80 ± 0.20	4.1 ± 0.3
$N_{\rm H}$ (cm^{-2})	(8.7 ± 0.4) × 10^{20}	3 × 10^{18}	10^{18}
χ^2_ν/d.o.f.	1.1/688	1.26/411	1.1/367

We based the EMD reconstruction on a subset of lines, among those identified in RGS spectra, with reliable flux measurements and emissivity curves (from the APED v1.2 database), and we employed the Markov-Chain Monte Carlo (MCMC) method by Kashyap & Drake (1998). The derived EMDs are plotted in Figure 4.

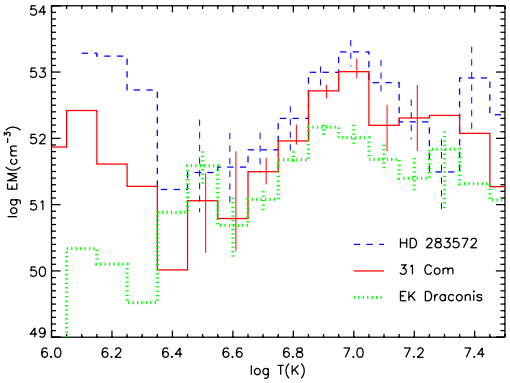

Figure 4. EM distributions derived with RGS data. Values without error bars are not statistically constrained by the MCMC algorithm.

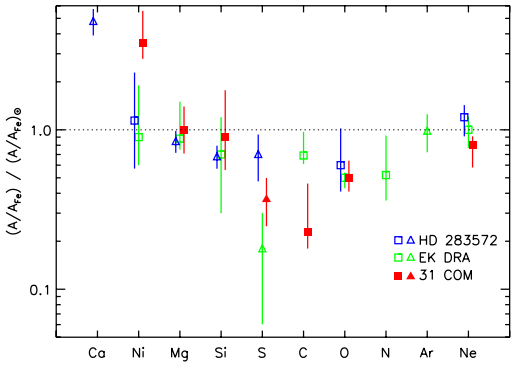

Figure 5. Element-to-iron abundance ratios, relative to solar values. For each star, squares refer to the RGS-derived ratios, while triangles to the pn-derived ones.

6. Abundances

Figure 5 shows the element-to-iron abundance ratios for the three stars (relative to the solar ones), derived from the RGS or from the pn best-fit models whenever the former values are not available; the elements are sorted by increasing FIP. The iron abundances of HD 283572, EK Dra and 31 Com (relative to the solar value) were estimated to be 0.7 ± 0.2, 1.2 ± 0.2 and 1.4 ± 0.2, respectively, by comparison of predicted and observed continuum emission level.

The patterns of abundances vs. FIP are similar in the cases of 31 Com and HD 283572, with an initial decrease down to a minimum around Carbon, followed by increasing abundances for elements with higher FIP (> 11 eV). This pattern is also similar to what found in the young active star AB Dor by Sanz-Forcada et al (2003), but it is less evident in the case of EK Dra.

7. Conclusions

A remarkable result of this work is the close similarity of the emission measure distributions of HD 283572 and 31 Com, which are the two stars with similar L_X as well, but F_X differing by a factor ~ 10. Both distributions have a well-defined peak at $T_p = 10^7$ K, with an ascending part ($\log T \sim 6.5 - 7$) proportional to $\sim T^5$. There is also evidence of a larger amount of plasma at $T > 10^{7.3}$ K in HD 283572 than in 31 Com. The EMD of EK Dra peaks at $\log T = 6.9$ and its ascending part ($\log T \sim 6.6 - 6.9$) can be approximated by a power law with a slope similar to that of HD 283572 and 31 Com.

Our interpretation of this result is that the coronae of these active stars are very similar in terms of dominant coronal magnetic structures, in spite of differences in the evolutionary phase, surface gravity and metallicity; moreover, L_X correlates better than F_X with the shape of the EMD and the total coronal emission measure of these stars.

Acknowledgements

L. S. acknowledges partial financial support from ESA for his partecipation to the CS 13 meeting.

References

Bowyer S., Drake J.J., Vennes S. 2000, ARA&A 38, 231
Favata F., Micela G. 2003, SSRv 108, 577F
Grevesse N., Noels A., Sauval A.J. 1992, in Coronal Streamers, Coronal Loops, and Coronal and Solar Wind Composition 305-308
Güdel M., Guinan E.F., Mewe R., Kaastra J.S., Skinner S.L. 1997, ApJ 479, 416
Kashyap V., Drake J.J. 1998, ApJ 503, 450
Piskunov N., Wood B.E., Linsky J.L., Dempsey R.C., Ayres T.R. 1997, ApJ 474, 315
Sanz-Forcada J., Maggio A., Micela G. 2003, A&A 408, 1087S
Scelsi L., Maggio A., Peres G., Gondoin P. 2004, A&A 413, 643
Strassmeier K.G., Rice J.B. 1998, A&A 339, 497
Walter F.M., Brown A., Linsky J.L. et al 1987, ApJ 314, 297